Three-parameter kinetics of a phase transition

A. I. Olemskoĭ and A. V. Khomenko

Sumy State University, 244007 Sumy, Ukraine
(Submitted 17 April 1996)
Zh. Éksp. Teor. Fiz. **110**, 2144–2167 (December 1996)

Using the Lorentz model we study the kinetics of first- and second-order phase transitions represented by an order parameter, a conjugate field, and a control parameter. We examine the various limiting cases in the ratios of the corresponding relaxation times. The phase portraits in various kinetic modes are studied both analytically and numerically. We show that oscillatory behavior result from a critical increase in the relaxation times of the order parameter and the conjugate field if the initial relaxation time of the control parameter is much longer that its value for other degrees of freedom. In the opposite case all phase trajectories rapidly converge to a universal section known as the "mainstream" (A. S. Zel'tser, T. K. Soboleva, and A. É. Filippov, JETP **81**, 193 (1995)). © *1996 American Institute of Physics.* [S1063-7761(96)01712-X]

1. INTRODUCTION

In recent years there has been an upsurge of interest in the kinetics of phase transitions (see the reviews in Refs. 1 and 2 and the literature cited therein). The main reason why considerable progress has been made in describing the space–time evolution of systems undergoing a phase transition lies in the scaling hypothesis, which was first used in the critical region.[3] But while in this region the scale on which the coordinate varies is limited to the correlation length $\xi\to\infty$, in describing the evolution of the new phase the role of the scale is taken by either the characteristic phase L of the antiphase domain (in describing the "Lifshitz foam"[4]) or the critical size R_c of formation (in the coalescence picture[5]). Within the scale-invariance hypothesis the structure factor $S(\mathbf{r},t)$ (in the case of coalescence, the probability distribution $P(R,t)$ over the formation sizes R) is represented in a universal manner as a function of the coordinate $\mathbf{r}$ and precipitation radius R measured on the respective scales. Scale invariance makes it possible to fix the time dependence of $L(t)$ and $R_c(t)$ and establish the asymptotic behavior of the correlator $S(r/L(t))$ for $r\ll L$ and for $r\gg L$ (see Refs. 1 and 2; in the Lifshitz–Slezov problem[5] not only can the asymptotic behavior of the distribution $P(R/R_c(t))$ be established but even the analytical form of the distribution proper can be derived). It was found that the form of $S(r/L)$ and $P(R/R_c)$ is insensitive to the choice of microscopic parameters (such as the interatomic interaction potential) and is determined entirely by the condition that the order parameter must be constant and by the dimensionalities d and n of the physical and order-parameter spaces (the Ising and Heisenberg models have $n=1$ and $n=\infty$, respectively). For example, the short-wave ($kL\gg 1$) asymptotic behavior of the spatial Fourier transform of the correlator $S(\mathbf{r},t)$ in the case of a conserved order parameter has the form of a generalized Porod law $S(\mathbf{k},t)\propto L^{-n}k^{-(d+n)}$ characterizing the presence of sharp phase boundaries.[1] In the limit $t\to\infty$, the domain size is determined by the relationship $L^{c+d-1}\propto t$, where $c=2$ holds for a conserved order parameter and $c=0$ for a nonconserved one, and the critical radius R_c^d of a coagulating system is proportional to t (Refs. 1 and 2).

The above shows that the universality of the phenomenological pattern of a phase transition is inherent not only in the thermodynamic behavior but also in the kinetic (dynamical, to be more precise) behavior. Recently Zel'tser *et al.*[6] discovered one more manifestation of the universality of the kinetic pattern of a phase transition. The researchers started from the fact that in the course of a phase transition the order parameter $\eta(t)$ may change in a nonautonomous manner. For instance, if striction effects are important, the ordering of the medium is accompanied by the emergence of a strain field conjugate to the order parameter.[1)] Usually it is assumed that both fields are able to follow the variations of the order parameter. For this to be the case the relaxation time τ_h of the conjugate field $h(t)$ must be much shorter than the corresponding quantity τ_η for the order parameter ($\tau_h\ll\tau_\eta$). Then we can easily show that the striction effect is reduced to the appearance of a long-range field that renormalizes the thermodynamic potential. Under certain conditions the effect of this renormalization is such that the phase transition slows down (or even stops).[6] This fact can be interpreted as a manifestation of the Le Chatelier principle, which reflects the presence of negative feedback between the order parameter and the conjugate field.

The universality of the kinetic pattern of a phase transition discovered by Zel'tser *et al.*[6] becomes evident if we assume that the system's behavior is determined not only by the order parameter but also by another thermodynamic degree of freedom, T, whose characteristic relaxation time τ_T is commensurate with the corresponding quantity τ_η for the order parameter. In this connection the researchers examined another mechanism of the Le Chatelier principle, i.e., caused by the heating of the region adjoining the precipitation of the phase formed as a result of rapid cooling of the system below the first-order phase transition point. Here the local value of the temperature in the region of the precipitation phase acts as the control parameter T. Reasoning heuristically, Zel'tser *et al.*[6] obtained a system of nonlinear differential equations for determining the functions $\eta(t)$ and $T(t)$. A study of the phase portrait $\eta(T)$ and the shape of the functions $\eta(t)$ and $T(t)$ shows that there are two areas in which the behavior of

 1063-7761/96/121180-13$10.00

the phase trajectories differs. In the first area both η and T evolve fairly rapidly with the passage of time, and the area has little effect on the kinetic behavior of the system. The behavior is fixed by the slow variation of $\eta(t)$ and $T(t)$ in the second area, whose position is determined by the proximity to the separatrix and which in Ref. 6 was aptly named the "mainstream." Thus, in the phase-portrait representation the universality of the kinetics of a phase transition manifests itself as a certain separatrix region (a line in the limit) whose position is independent of the microscopic details of the system's behavior.

Note that the argument of Ref. 6 is based specifically on model ideas, although we believe the conclusions to be of a more general nature. In this connection it is important to formulate the given problem in a setting not restricted by model considerations. The present paper attempts to do this.

The starting point of our approach is the synergetic concept of a phase transition. Within this concept a phase transition is realized as a result of the mutually coordinated behavior of three degrees of freedom: the order parameter $\eta(t)$, the conjugate field $h(t)$, and the control parameter $T(t)$ (see Ref. 7). As noted earlier, the variables in the first pair are linked by negative feedback. The basic assumption of the synergetic approach is that the positive feedback between the second pair, $\eta(t)$ and $T(t)$, can lead to self-organization of the system, which is the reason for the phase transition.

Mathematically, the simplest way to describe self-organizing systems is to use the well-known Lorentz scheme.[7] It consists of three differential equations that express the rates $\dot{\eta}$, $\dot{h}$, and $\dot{T}$ of variation of η, h, and T in terms of their values. A characteristic feature of these expressions is that they all contain dissipative terms whose values are inversely proportional to the corresponding relaxation times τ_η, τ_h, and τ_T. The usual approach to studying the thermodynamics of a phase transition is to adopt the adiabatic approximation $\tau_h, \tau_T \ll \tau_\eta$, which means that in the course of their evolution the conjugate field $h(t)$ and the control parameter $T(t)$ change so rapidly that they are able to follow the slow variation of the order parameter $\eta(t)$ (see Ref. 7). Here the evolution of the system is described by a (single) Landau–Khalatnikov equation in which the synergetic potential acts as the free energy. As a result the synergetic approach is reduced to the standard phenomenological scheme of a phase transition. The difference here is that in stochastic systems the self-organization process takes place in the high-temperature region, while in thermodynamic systems it takes place in the low-temperature region. In addition, while for thermodynamic systems the temperature of the medium coincides with that of the thermostat, for synergetic phase transitions the negative feedback between the order parameter and the conjugate field, which reflects the Le Chatelier principle, lowers the steady-state value of the control parameter in comparison to its value fixed by an external perturbation.

One can easily see that to describe the kinetic features of a phase transition that are found from model considerations[6] and yet remain in the realm of the synergetic approach, we must weaken the standard coordination principle,[7] assuming that not one but two hydrodynamic degrees of freedom have the greatest relaxation time. As a result the kinetics of a phase transition is represented by a system of two differential equations. Our main goal is to study the possible scenarios that second-order (Sec. 2) and first-order (Sec. 3) phase transitions follow. An essential merit of the synergetic approach is that, without resorting to limited model ideas, it allows for the action of a generalized Le Chatelier principle. In this sense the results of our investigation are fairly general. We find, in particular, that the Hamiltonian reproducing the nondissipative terms in the Lorentz equations has the simplest Fröhlich form.[8]

2. SECOND-ORDER PHASE TRANSITION

To simplify matters, we study the case of a nonconserved order parameter, for which there is no dependence on position. Then the initial system of Lorentz equations is[7]

$$\dot{e} = -\frac{\eta}{\tau_\eta} + g_\eta h, \tag{1}$$

$$\dot{h} = -\frac{h}{\tau_h} + g_h \eta T, \tag{2}$$

$$\dot{T} = \frac{T_0 - T}{\tau_T} - g_T \eta h. \tag{3}$$

Here the dot stands for a derivative with respect to t (time); τ_η, τ_h, and τ_T are the relaxation times of the order parameter $\eta(t)$, the conjugate field $h(t)$, and the control parameter $T(t)$; g_η, g_h, and g_T are positive coupling constants; and T_0 is the thermostat temperature. A characteristic feature of the system (1)–(3) is the linearity of the right-hand side of Eq. (1) in the order parameter and the corresponding nonlinearities in Eqs. (2) and (3). The first terms describe the relaxation of the system to the steady-state values $\eta = 0$, $h = 0$, and $T = T_0$, while the second terms describe the relationship between the different hydrodynamic modes. The minus in front of the nonlinear term in (3) reflects the action of the Le Chatelier principle, and the plus in front of ηT in (2) reflects the presence of positive feedback between $\eta(t)$ and $T(t)$, which is the reason for self-organization.

If $\tau_h, \tau_T \ll \tau_\eta$, we can neglect the fluctuations in $h(t) \approx h(\eta(t))$ and $T(t) \approx T(\eta(t))$, setting $\dot{h} = 0$ and $\dot{T} = 0$ in Eqs. (2) and (3). This leads to equations expressing the conjugate field and the control parameter in terms of the order parameter:

$$h = A_h T_0 \eta \left(1 + \frac{\eta^2}{\eta_m^2}\right)^{-1}, \tag{4}$$

$$T = T_0 \left(1 + \frac{\eta^2}{\eta_m^2}\right)^{-1}, \tag{5}$$

where

$$\eta_m^{-2} \equiv A_T A_h, \quad A_i \equiv \tau_i g_i, \quad i = \eta, h, T. \tag{6}$$

For $\eta \ll \eta_m$ Eq. (4) has a linear form characterized by a susceptibility $\chi = (A_h T_0)^{-1}$. As the order parameter increases to $\eta = \eta_m$, the $h(\eta)$ dependence becomes saturated, and for $\eta > \eta_m$ the dependence becomes decreasing, which has no

physical meaning. This implies that the constant η_m defined in (6) has the meaning of the maximum value of the order parameter. As for Eq. (5), it describes the decrease in the control parameter from the maximum value T_0 at $\eta=0$ to the minimum value $\frac{1}{2}T_0$ at $\eta=\eta_m$. Obviously, the decreasing nature of the T vs η dependence is a manifestation of the Le Chatelier principle.

Plugging (4) into (1), we arrive at an equation of the Landau–Khalatnikov form:

$$\tau_h\dot{\eta}=-\frac{\partial V}{\partial \eta}, \tag{7}$$

where the synergetic potential V has the form

$$V=\frac{\eta^2}{2}\left\{1-\frac{T_0}{T_c}\left(\frac{\eta}{\eta_m}\right)^{-2}\ln\left[1+\left(\frac{\eta}{\eta_m}\right)^2\right]\right\}, \tag{8}$$

$$T_c\equiv(A_\eta A_h)^{-1}. \tag{9}$$

If the thermostat temperature T_0 is lower than the critical value T_c defined by Eq. (9), V monotonically increases with η and has its minimum at point $\eta_0=0$. Here the system does not become ordered. In the supercritical region $T_0>T_c$ the synergetic potential acquires a minimum at the nonzero value of the order parameter[2)]

$$\eta_0=\eta_m\sqrt{\theta-1}, \quad \theta\equiv\frac{T_0}{T_c}. \tag{10}$$

This means that when the system rapidly proceeds to the region where the dimensionless thermostat temperature θ is greater than unity, it takes

$$\tau=\tau_h(\theta-1)^{-1} \tag{11}$$

units of time for the order parameter to reach the steady-state value (10). Here the time dependence of η has the usual Debye form

$$\eta=\eta_0(1-e^{-t/\tau}). \tag{12}$$

2.1. The case $\tau_h\ll\tau_\eta,\tau_T$

As we did earlier, we can set $\dot{h}=0$ in (2), which yields the following relationship:

$$h=A_hT\eta. \tag{13}$$

Plugging it into the remaining equations (1) and (3) and using the scales η_m, T_c, and τ_η for the time variation of the order parameter and the control parameter, we arrive at the following system of equations:

$$\dot{\eta}=-\eta(1-T), \tag{14}$$

$$\dot{T}=\tau^{-1}[\theta-T(1+\eta^2)]. \tag{15}$$

Its behavior is fixed by two parameters,

$$\theta\equiv\frac{T_0}{T_c}, \quad \tau\equiv\frac{\tau_T}{\tau_\eta}, \tag{16}$$

with the first defining the degree of excitation of the system, and the second the ratio of the relaxation times of the control parameter and the order parameter. In the limit $\tau\ll1$ the right-hand side of Eq. (15) assumes values so large that we can set $\dot{T}=0$ in the left-hand side, and after the resulting dependence (5) is substituted in (14) we arrive at the above adiabatic approximation represented by Eqs. 7–9.

Generally, the standard analysis[9] of the system (14) and (15) shows that the phase portrait is marked by the presence of two singular points, $D(T_0,0)$ and $O(T_c,\eta_0)$, with coordinates $T=T_0,\eta=0$ and $T=T_c,\eta=\eta_0$, respectively, and with η_0 defined in (10). The corresponding Lyapunov exponents are

$$\lambda_D=\frac{1}{2}[(\theta-1)-\tau^{-1}]$$
$$\times\{1\pm\sqrt{1+4\tau^{-1}(\theta-1)[(\theta-1)-\tau^{-1}]^{-2}}\}, \tag{17}$$

$$\lambda_O=-\frac{\theta}{2\tau}\left[1\pm\sqrt{1-8\tau\frac{\theta-1}{\theta^2}}\right]. \tag{18}$$

We see that in the subcritical region ($\theta<1$) the point D is a stable node, while the point O is not realized. This means that with the passage of time the system evolves to the stationary disordered state corresponding to point D, according to the phase portrait depicted in Fig. 1a. An increase in the parameter $\tau=\tau_T/\tau_\eta$ leads to the trajectories becoming twisted around point D, i.e., as the inertia of variation of the control parameter grows in comparison to that of the order parameter, the tendency toward an oscillatory mode increases.

As the phase portrait in Fig. 2 shows, this tendency is realized in full in the transition to the supercritical region $\theta>1$, where D is transformed into a saddle point and an additional point O emerges. For values of the parameter τ limited from above by

$$\tau_c=\frac{\theta^2}{8(\theta-1)}, \tag{19}$$

the point O is a stable node, and as τ becomes greater than τ_c this point becomes a stable focus.

Thus, in the supercritical region $1<\theta\leqslant2$ for $\tau_\eta\ll\tau_T$ an oscillatory mode with a characteristic frequency

$$\omega=\frac{\theta}{2\tau_T}\sqrt{8\tau\theta^{-2}(\theta-1)-1} \tag{20}$$

and a damping constant

$$\alpha=\frac{\theta}{2\tau_T} \tag{21}$$

sets in (see Fig. 2c). With the temperature growing in the interval $1<\theta<2$ the values of ω and α grow and the critical relaxation-time ratio (19) decreases. In other words, excitation of the system expedites the appearance of damped oscillations, as expected. However, as Fig. 2 shows, the increase in the parameter $\tau=\tau_T/\tau_\eta$ is the largest factor in the manifestation of an oscillatory mode.

The opposite limit $\tau_T\ll\tau_\eta$ corresponds to the adiabatic approximation, which represents the standard pattern of a phase transition. According to Fig. 2, a decrease in the parameter τ to zero leads to a section MOD appearing in the phase portrait to which all the trajectories finally converge. As the time curves in Fig. 3a show, an image point rapidly

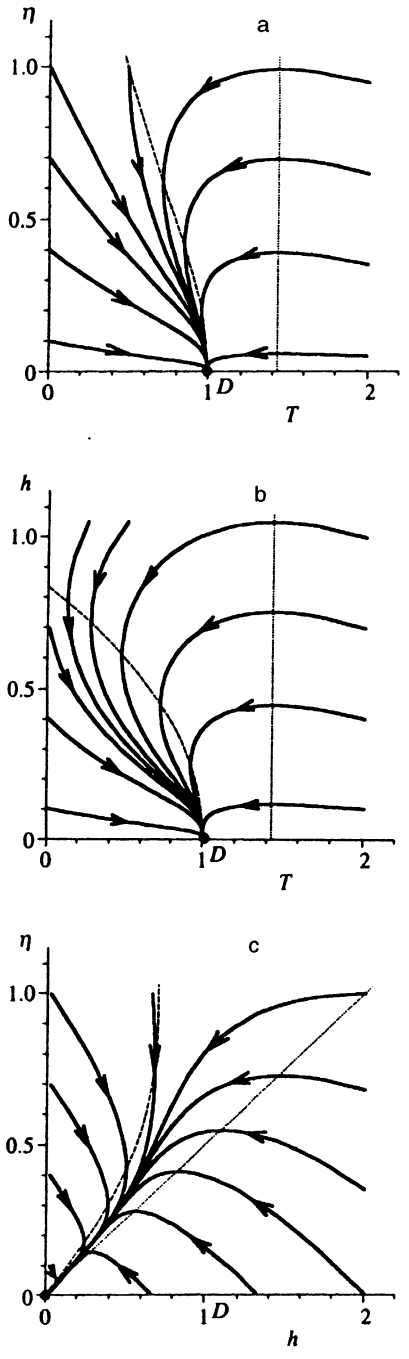

FIG. 1. Phase portraits of the disordered phase ($T_0=0.7T_c$) for a second-order phase transition: (a) $\tau_h \ll \tau_\eta = \tau_T$, (b) $\tau_\eta \ll \tau_h = \tau_T$, and (c) $\tau_T \ll \tau_h = \tau_\eta$. Here and in all figures that follow the temperature is measured in units of T_0; a dotted line indicates the points at which the phase trajectories have a vertical tangent, and a dashed line indicates the points at which the phase trajectories have a horizontal tangent.

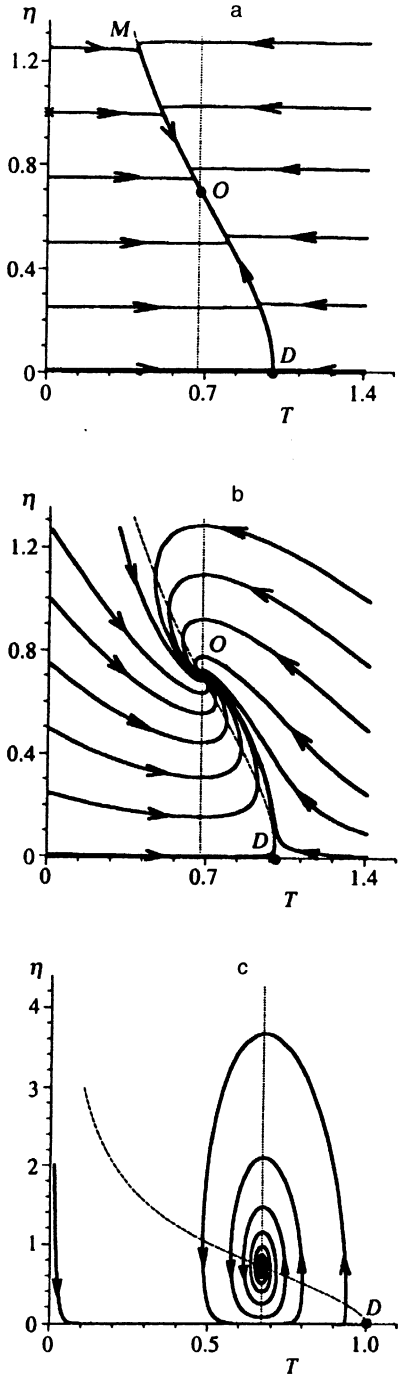

FIG. 2. Phase portraits of the ordered phase ($T_0=1.5T_c$) for a second-order phase transition: (a) $\tau_h \ll \tau_\eta = 10^2\tau_T$, (b) $\tau_h \ll \tau_\eta = \tau_T$, (c) $\tau_h \ll \tau_T = 10^2\tau_\eta$.

moves along a trajectory lying outside the *MOD* section, while when such a point finds itself within this section, its motion becomes rapidly retarded, and the smaller the nonadiabaticity parameter τ the stronger the retardation. Obviously, the section *MOD* corresponds to an attractive set, which in Ref. 6 was named the "mainstream." The universality of the kinetic pattern of a phase transition manifests itself in a situation in which, irrespective of the initial conditions for $\tau \to 0$, the system promptly reaches the *MOD* section, whose position is independent of the microscopic details of the section's structure, and slowly evolves along this universal trajectory.

2.2. The case $\tau_\eta \ll \tau_h, \tau_T$

Setting $\dot{\eta}=0$ in (1), we arrive at the relationship

$$\eta = A_\eta h, \tag{22}$$

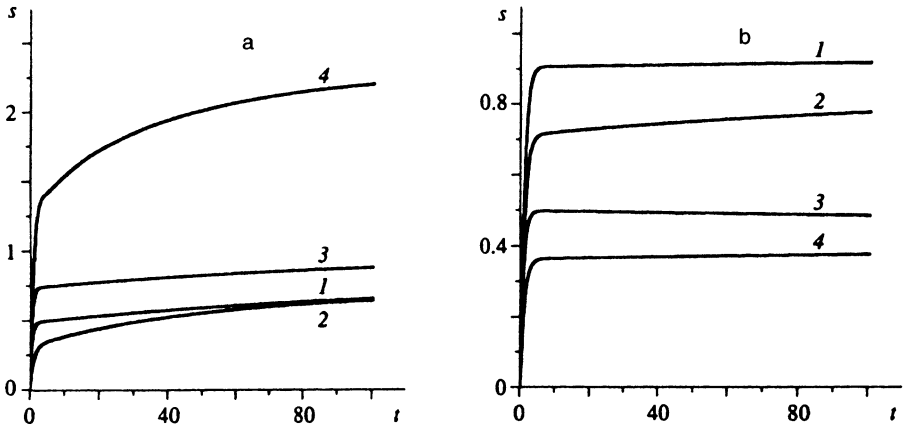

FIG. 3. The time dependence of the path s traversed by an image point moving along a phase trajectory: (a) a second-order phase transition (curve *1* corresponds to the phase portrait in Fig. 2a, curve *2* to the phase portrait in Fig. 4a, curve *3* to the phase portrait in Fig. 5a, and curve *4* to the phase portrait in Fig. 5c), and (b) a first-order phase transition (curve *1* corresponds to the phase portrait in Fig. 7a, curve *2* to the phase portrait in Fig. 8a, curve *3* to the phase portrait in Fig. 9a, and curve *4* to the phase portrait in Fig. 9c). The origin of s is marked by $\times$ in the respective diagrams.

which when plugged into (2) and (3) yields the following system of equations:

$$\dot{h}=-h(1-T), \tag{23}$$

$$\dot{T}=\tau^{-1}[\theta-(T+h^2)], \tag{24}$$

where the quantities h, T, and t are measured in units of h_m, T_c, and τ_h, respectively, and we have introduced the characteristic parameters

$$\tau\equiv\frac{\tau_T}{\tau_h},\quad h_m\equiv\frac{\eta_m}{A_\eta}=\frac{1}{A_\eta\sqrt{A_hA_T}}. \tag{25}$$

As in the first case, the phase portrait is determined by the presence singular points, $D(T_0,0)$ and $O(T_c,h)$, where

$$h_0=h_m\sqrt{\theta-1} \tag{26}$$

determines the steady-state value of the conjugate field. The Lyapunov exponents have the form

$$\lambda_D=\frac{1}{2}[(\theta-1)-\tau^{-1}]\times\left\{1\pm\sqrt{1+4\tau^{-1}\frac{\theta-1}{[(\theta-1)-\tau^{-1}]^2}}\right\}, \tag{27}$$

$$\lambda_O=-\frac{1}{2\tau}[1\pm\sqrt{1-8\tau(\theta-1)}]. \tag{28}$$

As above, the point D for $\theta<1$ is an attractive node, while for $\theta>1$ it is a saddle point. Point O is realized only in the ordered region $\theta>1$, where it is an attractive node for small values of the parameter τ and a stable focus if τ exceed the critical value

$$\tau_c=\frac{1}{8(\theta-1)}. \tag{29}$$

The corresponding values for the oscillation frequency and the damping constant are

$$\omega=\frac{1}{2\tau_T}\sqrt{8\tau(\theta-1)-1}, \tag{30}$$

$$\alpha=\frac{1}{2\tau_T}. \tag{31}$$

As the temperature θ rises, τ_c decreases and the frequency ω grows, but α remains unchanged.

This analysis and the shape of the phase portraits in Fig. 4 show that, as in the previous case, for large values of the parameter τ the mode damping sets in (Fig. 4c), while as τ decreases to values much smaller than unity, dissipative relaxation sets in (Fig. 4a). Similarly, in the adiabatic limit $\tau\to0$ the kinetic behavior becomes universal, which is reflected in Fig. 4a by the presence of a special section MOD on which the system slowly evolves to the stationary point O.

2.3. The case $\tau_T\ll\tau_\eta,\tau_h$

Setting $\dot{T}=0$ in (3), we arrive at the relationship

$$T=T_0-A_T\eta h, \tag{32}$$

which when inserted in (1) and (2) yields the following system of equations:

$$\dot{\eta}=-\eta+h, \tag{33}$$

$$\dot{h}=\tau^{-1}[\theta\eta-h(1+\eta^2)], \tag{34}$$

where the quantities η, h, and t are measured in units of η_m, h_m, and τ_η, respectively, and where we have introduced the relaxation-time ratio

$$\tau\equiv\frac{\tau_h}{\tau_\eta}. \tag{35}$$

The phase portrait of the system has two singular points, $D(0,0)$ and $O=(h_m\sqrt{\theta-1},\eta_m\sqrt{\theta-1})$ (Fig. 5), with the second point being present only in the region $\theta>1$. The corresponding Lyapunov exponents have the form

$$\lambda_D=-\frac{1}{2}(1+\tau^{-1})\times[1\pm\sqrt{1+4\tau^{-1}(1+\tau^{-1})^{-2}(\theta-1)}], \tag{36}$$

$$\lambda_O=-\frac{1+\tau^{-1}\theta}{2}\left[1\pm\sqrt{1-8\tau\frac{\theta-1}{(\theta+\tau)^2}}\right]. \tag{37}$$

For $\theta<1$ the point D is a stable node, and the transition to the supercritical region $\theta>1$ transforms it into a saddle

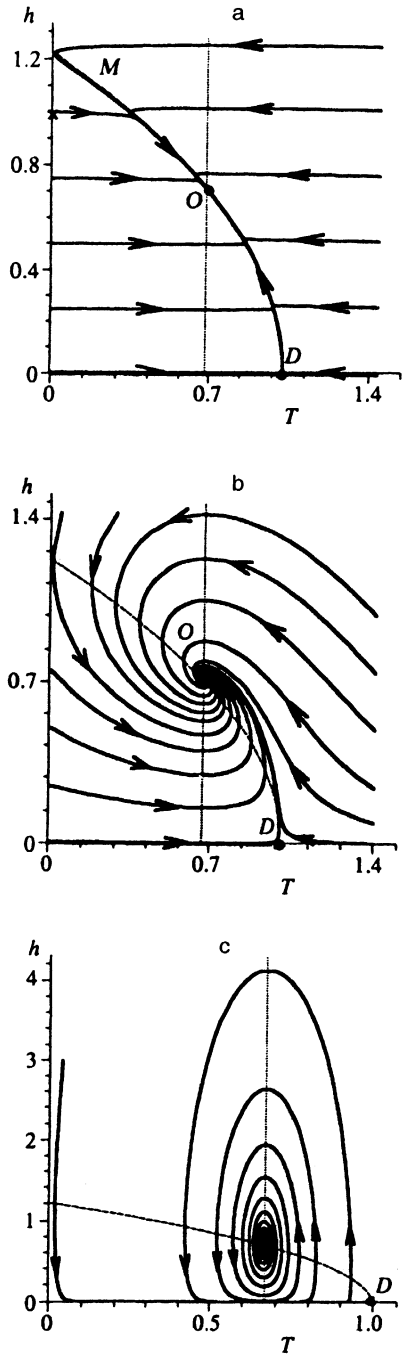

FIG. 4. Phase portraits of the ordered phase ($T_0 = 1.5T_c$) for a second-order phase transition: (a) $\tau_\eta \ll \tau_h = 10^2 \tau_T$, (b) $\tau_\eta \ll \tau_h = \tau_T$, and (c) $\tau_\eta \ll \tau_T = 10^2 \tau_h$.

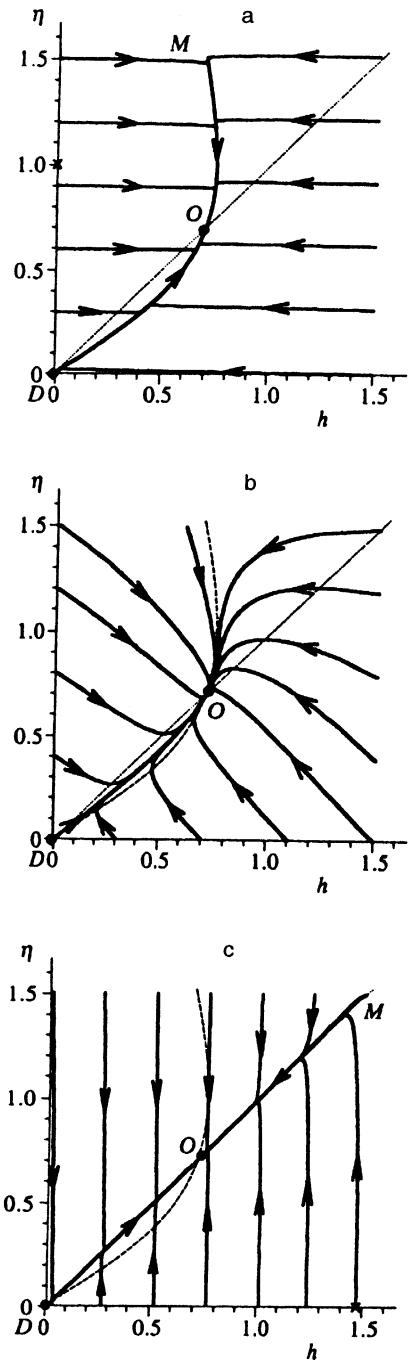

FIG. 5. Phase portraits of the ordered phase ($T_0 = 1.5T_c$) for a second-order phase transition: (a) $\tau_T \ll \tau_\eta = 10^3 \tau_h$, (b) $\tau_T \ll \tau_\eta = \tau_h$, and (c) $\tau_T \ll \tau_h = 10^2 \tau_\eta$.

point. Point O, which characterizes the ordered phase, is an attractive focus for values of τ belonging to the interval (τ_-, τ_+), where

$$\tau_\pm = 3\theta - 4 \pm \sqrt{8(\theta-1)(\theta-2)}, \tag{38}$$

and an attractive node outside the interval. The characteristic values of the frequency,

$$\omega = \frac{1}{2\tau_h}\sqrt{8\tau(\theta-1) - (\tau+\theta)^2}, \tag{39}$$

and the damping constant,

$$\alpha = \frac{\tau+\theta}{2\tau_h}, \tag{40}$$

are comparable for all values of θ and τ. Here, in contrast to the cases considered earlier, the oscillatory mode is, for all practical purposes, absent.

According to the phase portraits in Fig. 5, the kinetic behavior exhibits its universal nature both for $\tau_h \ll \tau_\eta$ and for $\tau_h \gg \tau_\eta$. In the first case the universal section is reached due

to the rapid variation of the conjugate field $h(t)$ with the order parameter $\eta(t)$ remaining practically unchanged (Fig. 5a), while in the second case the opposite is true—the order parameter changes very rapidly and the conjugate field remains almost the same (Fig. 5c). In the intermediate region $\tau_\eta \sim \tau_h$ universality manifests itself only for small initial values $h(0)$ and $\eta(0)$, i.e., $h(0) \ll h_0$ and $\eta(0) \ll \eta_0$ (Fig. 5b). Note that in contrast to the previous cases the universal section of the phase trajectories has an increasing nature rather than a decreasing one.

3. FIRST-ORDER PHASE TRANSITION

The simplest way to proceed from the above case of a second-order phase transition to that of a first-order one is to replace the constant relaxation time τ_η in (1) by the following dependence:[7]

$$\frac{1}{\tau_\eta}=\frac{1}{\tau_0}\left[1+\frac{\kappa}{1+(\eta/\eta_\tau)^2}\right], \tag{41}$$

characterized by the positive constants τ_0, κ, and η_τ. Then, within the adiabatic approximation $\tau_h, \tau_T \ll \tau_0$, the Lorentz system of equations (1)–(3) is reduced to Eq. (7), in which τ_η is denoted by τ_0, and the synergetic potential (8) assumes the form

$$V=\frac{\eta^2}{2}\left\{1-\frac{T_0}{T_{c0}}\left(\frac{\eta}{\eta_m}\right)^{-2}\ln\left[1+\left(\frac{\eta}{\eta_m}\right)^2\right]\right\} + \frac{\kappa\eta_\tau^2}{2}\ln\left[1+\left(\frac{\eta}{\eta_\tau}\right)^2\right], \tag{42}$$

where $T_{c0}\equiv(\tau_0\tau_h g_\eta g_h)^{-1}$. For low values of T_0 the V vs η dependence has a monotonically increasing shape with its minimum at point $\eta=0$. At

$$T_c^0=T_{c0}\left[1+\frac{\eta_\tau^2}{\eta_m^2}(\kappa-1)+2\frac{\eta_\tau}{\eta_m}\sqrt{\kappa\left(1-\frac{\eta_\tau^2}{\eta_m^2}\right)}\right] \tag{43}$$

a plateau appears, which for $T_0>T_c^0$ is transformed into a minimum corresponding to nonzero values of the order parameter η_0 and a maximum separating the ordered- and disordered-phase minima. When the temperature T_0 increases still further, the ordered-phase minimum grows deeper and the height of the interphase barrier decreases, vanishing at the critical temperature

$$T_c=T_{c0}(1+\kappa). \tag{44}$$

The steady-state value of the order parameter has the form

$$\eta_0=\eta_{00}\sqrt{\sqrt{1+\left(\frac{\eta_m\eta_\tau}{\eta_{00}^2}\right)^2\frac{T_0-T_c}{T_{c0}}}-1} \approx \frac{\eta_m\eta_\tau}{\eta_{00}}\sqrt{\frac{T_0-T_c}{2T_{c0}}}, \tag{45}$$

where the second equality is written for the case $T_0-T_c \ll T_{c0}$, and

$$\eta_{00}^2\equiv\frac{1}{2}\left[\left(1-\frac{T_0}{T_{c0}}\right)\eta_m^2+(1+\kappa)\eta_\tau^2\right]. \tag{46}$$

For $T_0>T_c$ the V vs η dependence has the same shape as for a second-order phase transition (see Sec. 2). Note that the energy barrier inherent in a first-order phase transition manifests itself only if the parameter $\alpha\equiv\eta_\tau/\eta_m$ is no greater than unity.

Next we measure η, $\hbar$, and T in units of η_m, h_m, and T_c (see Eqs. (6), (25) and (9)) and, as in the case of a second-order transition, examine the various limiting ratios of the relaxation times τ_0, τ_h, and τ_T, with the effective relaxation time τ_η in Eq. (1) given by (41).

3.1. The case $\tau_h \ll \tau_0, \tau_T$

Setting $\dot{h}=0$ in (2), we can write (13) as $h=T\eta$. Plugging this into Eq. (1) yields the following expression (time is measured in units of τ_0):

$$\dot{\eta}=-\eta\left[1-T+\frac{\kappa}{1+\eta^2/\alpha^2}\right], \tag{47}$$

which differs from (14) by the presence of the last term. The second equation, which follows from (3), has the same form (15) as above.

The phase portrait of the system (47) and (15) has three singular points, $D(\theta,0)$, $O(T_-,\eta_-)$, and $S(T_+,\eta_+)$, where the characteristic values $T_\pm$ and $\eta_\pm$ are given by the following equations:

$$T_\pm=\frac{1-\beta^2\pm\sqrt{(1-\beta^2)^2-\theta(1-\alpha^2)}}{1-\alpha^2}, \tag{48}$$

$$\eta_\pm=\sqrt{\frac{\theta-T_\pm}{T_\pm}}, \tag{49}$$

$$\beta^2\equiv\frac{1}{2}[1-\theta+\alpha^2(1+\kappa)], \quad \alpha\equiv\frac{\eta_\tau}{\eta_m}, \quad \theta\equiv\frac{T_0}{T_{c0}}. \tag{50}$$

Here we have introduced the parameter $\beta\equiv\eta_{00}/\eta_m$, where η_{00} stands for the characteristic value of the order parameter (46). Point D corresponds to a Lyapunov exponent that differs from (17) in that $\theta-\theta_c$ is substituted for $\theta-1$, where in accordance with (44) the quantity $\theta_c=1+\kappa$ defines a spinodal point. Hence, as in the case of a second-order phase transition, for $\theta<\theta_c$ the point D is a stable node, while for $\theta>\theta_c$ it is a saddle point. The Lyapunov exponents of the points $O(T_-,\eta_-)$ and $S(T_+,\eta_+)$ are expressed in terms of their coordinates (48) and (49) as follows:

$$\lambda_\pm=\lambda_0(1\pm\sqrt{1+\Delta}),$$

$$\lambda_0=\frac{\theta-T_\pm}{\kappa\alpha^2T_\pm}(T_\pm-1)^2-\frac{\theta}{2\tau T_\pm},$$

$$\lambda_0^2\Delta=\frac{2}{\tau}(\theta-T_\pm)\left[\frac{\theta(1-T_\pm)^2}{\alpha^2\kappa T_\pm^2}-1\right]. \tag{51}$$

In the interval $T_c^0<T<T_c$ in which a first-order phase transition is realized, S is a saddle point and O an attractive node or focus.

We see that as the thermostat temperature T_0 grows, the phase portrait of the system changes in the following way (Fig. 6). For $T_0<T_c^0$ when the dependence (42) has a monotonically increasing form, the points S and O are absent and

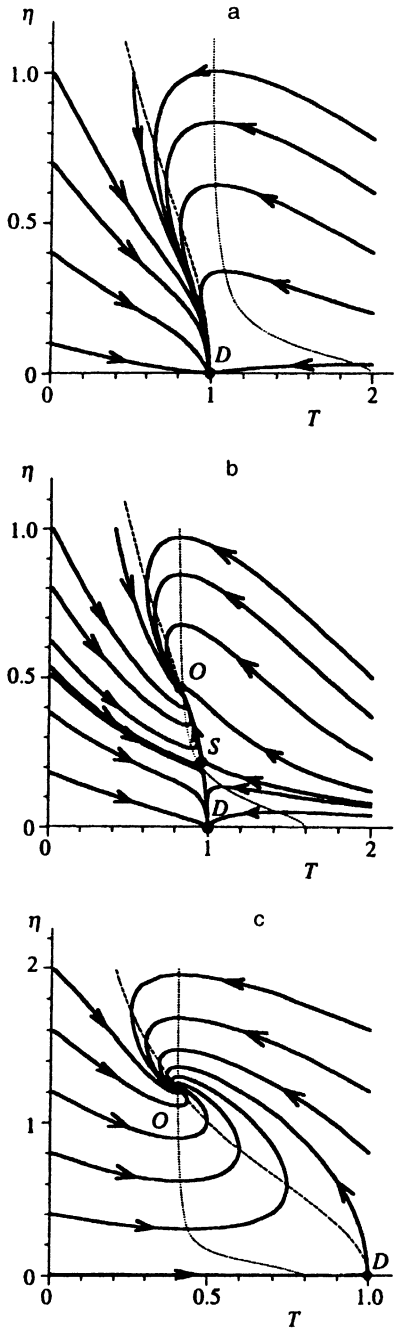

FIG. 6. Variation in the shape of phase portraits with temperature for a first-order phase transition ($\kappa=1$, $\alpha=0.1$, and $\tau_h \ll \tau_0 = \tau_T$): (a) $T_0 = T_{c0}$, (b) $T_0 = 1.25T_{c0}$, and (c) $T_0 = 2.5T_{c0}$.

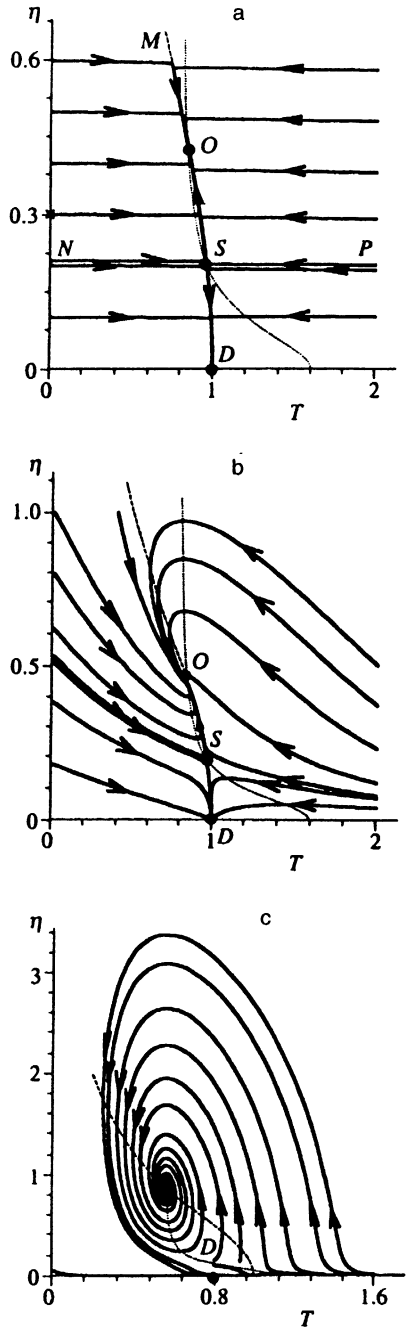

FIG. 7. Phase portraits for a first-order phase transition ($\kappa=1$ and $\alpha=0.1$): (a) $T_0 = 1.25T_{c0}$ and $\tau_h \ll \tau_0 = 10^2\tau_T$, (b) $T_0 = 1.25T_{c0}$ and $\tau_h \ll \tau_0 = \tau_T$, and (c) $T_0 = 1.8T_{c0}$ and $\tau_h \ll \tau_T = 10\tau_0$.

D is a stable node corresponding to the disordered phase. Here the portrait resembles that of a second-order phase transition (see Fig. 1a). When the temperature exceeds the critical value (43), the system undergoes a bifurcation, which consists in the appearance of a saddle point S and a stable node/focus O determined by the coordinates (48) and (49). As the thermostat temperature T_0 grows, the saddle point corresponding to an energy barrier in the V vs η dependence approaches the node D, and at T_c absorbs it. A further rise in temperature leads to a situation corresponding to the ordered phase for a second-order phase transition.

Figure 7 shows how the phase portrait of the ordered phase ($T_c^0 < T_0 < T_c$) varies with the relaxation time ratio $\tau = \tau_T/\tau_0$. Comparing it with Fig. 2, we see that in the neighborhood of O the behavior of the phase portrait is practically the same as for a second-order phase transition: in the adiabatic limit $\tau_T \ll \tau_0$ the trajectories rapidly converge to the universal section MOS (Fig. 7a), while in the opposite limit $\tau_T \gg \tau_0$ damped oscillations set in (Fig. 7c). The only difference is the appearance of a separatrix for small values of the order parameter, which is due to the presence of a barrier in the V vs η dependence. Studies of the time dependence of

the path s traversed by an image point moving along a trajectory show (see Fig. 3b) that, as in the case of a second-order phase transition, a slowdown occurs within the mainstream region MOS, which corresponds to the neighborhood of the ordered-phase minimum on the V vs η dependence.

These features of the kinetic behavior of the system can be understood by studying the dependence of the synergetic potential V on the values of the quantities η and T, which parametrize the behavior of the system. Here the reasoning should be based on the fact that in the course of its evolution the system stays mostly in the neighborhood of the extrema on the $V(\eta,T)$ dependence. Since the time of relaxation along each of the η,T axes is inversely proportional to the curvature of $V(\eta,T)$ along the respective axis,[3)] the condition $\tau_T \ll \tau_0$ means that the $V(\eta,T)$ dependence changes much faster along the T axis than it does along the η axis. As a result the surface of the function $V(\eta,T)$ has a narrow trough along the universal trajectory determined by the T vs η dependence (5). As Fig. 7a shows, the system rapidly slides down into the trough along the T axis, corresponding to the larger curvature. It is the presence of this trough that guarantees the universal nature of the kinetic behavior, since near the extrema the $V(\eta,T)$ dependence is always shaped like a parabola:

$$V \approx V(\eta_e,T_e)+\frac{\chi_\eta^{-1}}{2}(\eta-\eta_e)^2+\frac{\chi_T^{-1}}{2}(T-T_e)^2, \qquad (52)$$

where η_e and T_e determine the position of an extremum, and the susceptibilities χ_η and χ_T determine its curvature.

In view of what has been said it might seem that in the limit $\tau_0 \ll \tau_T$, which is the opposite of the adiabatic limit, the $V(\eta,T)$ dependence should also acquire a trough, with the result that there is no explanation of the nature of the damped-oscillation mode shown in Fig. 7c. One must bear in mind, however, that near the minimum in the $V(\eta,T)$ dependence the susceptibilities χ_η and χ_T in (52) are related to the relaxation times τ_η and τ_T in different ways: $\chi_T \propto \tau_T$ and $\chi_\eta \propto \tau_0|\theta-\theta_c|^{-1}$. Since $|\theta-\theta_c| \ll 1$ holds, the curvature $\chi_\eta^{-1} \propto \tau_0^{-1}|\theta-\theta_c|$ of the parabola (52) along the η axis proves to be comparable to the curvature $\chi_T^{-1} \propto \tau_T^{-1}$ of the $V(\eta,T)$ dependence along the T axis, notwithstanding the smallness of τ_0. In other words, in the $\tau_0 \ll \tau_T$ limit and near the ordered-phase minimum, the $V(\eta,T)$ dependence resembles a paraboloid with curvatures that have small (and similar) values along the η and T axes. As a result the image point, while sliding down into the minimum, may perform rotations along the paraboloid's surface. Obviously, such rotations represent the damped oscillations depicted in Fig. 7c.

Note that this critical increase in the susceptibility χ_η in (52) is of an essentially thermodynamic nature[11] and does not manifest itself near the maximum on the $V(\eta,T)$ dependence. This explains the absence of twisting in the separatrix in the $\tau_0 \ll \tau_T$ limit (see Fig. 7c).

Concluding this section, we note that although the expressions in (51) are cumbersome, they allow finding an analytical expression for the critical value τ_c of the relaxation-time ratio $\tau=\tau_T/\tau_0$ starting at which the point $O(T_-,\eta_-)$ is transformed from node to focus (see Eq. (19)). But since this analytical expression proves to be extremely cumbersome, we do not give it here.

3.2. The case $\tau_0 \ll \tau_h, \tau_T$

From the analytical point of view this is the most difficult case of all since substituting the effective relaxation time (41) into the initial equation (1), where we must set $\dot{\eta}=0$, leads not to the linear relationship (22) but to a cubic equation (see Refs. 10 and 11). It is convenient to write the solution of this equation in the form

$$3\eta = h + \eta_+(h) + \eta_-(h), \qquad (53)$$

where we have introduced the functions

$$\eta_\pm(h)=\left\{h(h^2+h_1^2)\pm 3\alpha\sqrt{3[(h^2+h_2^2)^2+h_3^4]}\right\}^{1/3} \qquad (54)$$

and constants h_1, h_2, and h_3 defined by the equations

$$h_1^2 \equiv \frac{9}{2}\alpha^2(2-\kappa), \quad h_2^2 \equiv \frac{1}{8}\alpha^2[36(2-\kappa)-(8-\kappa)^2],$$

$$h_3^2 \equiv \frac{1}{8}\alpha^2\sqrt{\kappa(8-\kappa)^3}, \quad \alpha \equiv \frac{\eta_\tau}{\eta_m}. \qquad (55)$$

Inserting (53) in Eqs. (2) and (3) reduces the latter to the following form (cf. Eqs. (23) and (24)):

$$\dot{h} = -h + \tfrac{1}{3}T[h+\eta_+(h)+\eta_-(h)], \qquad (56)$$

$$\tau\dot{T} = (\theta-T) - \tfrac{1}{3}h[h+\eta_+(h)+\eta_-(h)], \qquad (57)$$

where time is measured in units of τ_h and we have introduced the relaxation-time ratio $\tau \equiv \tau_T/\tau_h$.

Although there is no way to find the singular points or the corresponding Lyapunov exponents analytically, a numerical study of the phase portrait (Fig. 8) shows that the system behavior coincides with that studied in Sec. 3.1. Comparing the phase portrait with that of a second-order phase transition (see Fig. 4), we note the appearance of a separatrix in the region of values of T and h corresponding to the energy barrier separating the ordered and disordered phases, as in the case in Sec. 3.1.

If we follow the lines of reasoning of the previous case, we can easily see that for $\tau_T \ll \tau_h$, when the universality of the system's kinetic behavior manifests itself in full (Fig. 8a), the $V(h,T)$ dependence has a narrow trough along the universal section of the trajectories. The presence of a damped mode in the opposite limiting case $\tau_T \gg \tau_h$ (Fig. 8c) points to a critical increase in the susceptibility $\chi_h \propto \tau_h|\theta-\theta_c|^{-1}$ corresponding to the conjugate field. Obviously, the initial reason for such an increase is the critical rise in the susceptibility $\chi_\eta \propto \tau_0|\theta-\theta_c|^{-1}$ corresponding to the order parameter. It is the existence of the stringent function relationship (53) between $\eta(t)$ and $h(t)$ (for a second-order phase transition it assumes the linear form (22)) that ensures the rise in the susceptibility corresponding to the conjugate field.

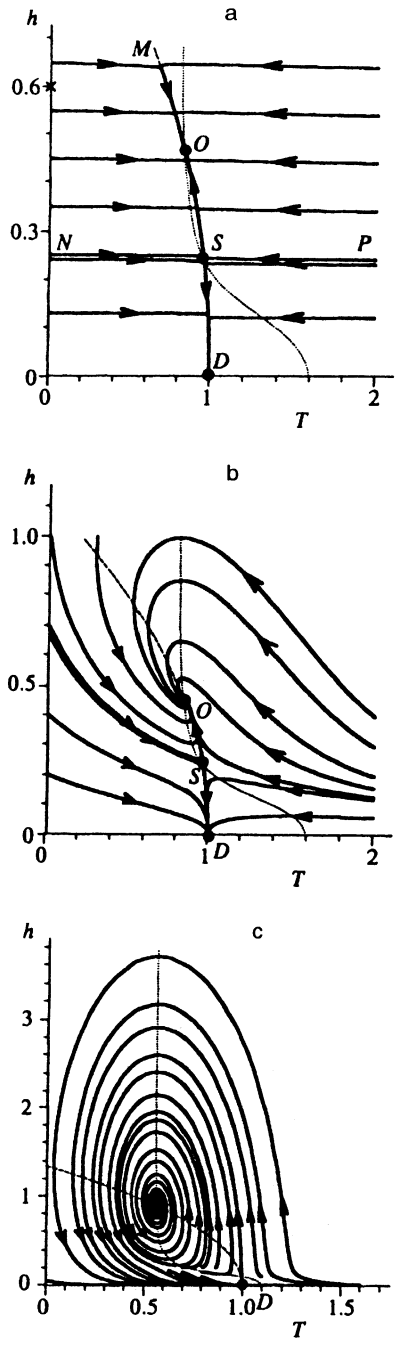

FIG. 8. Phase portraits for a first-order phase transition ($\kappa=1$ and $\alpha=0.1$): (a) $T_0=1.25T_{c0}$ and $\tau_0\ll\tau_h=10^2\tau_T$, (b) $T_0=1.25T_{c0}$ and $\tau_0\ll\tau_h=\tau_T$, and (c) $T_0=1.8T_{c0}$ and $\tau_0\ll\tau_T=10\tau_h$.

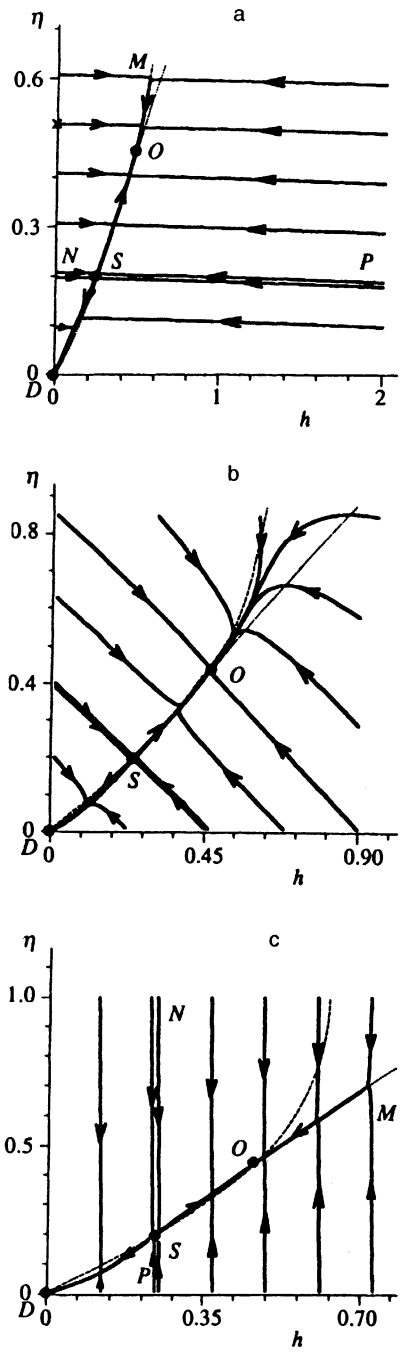

FIG. 9. Phase portraits for a first-order phase transition ($\kappa=1$, $\alpha=0.1$, and $T_0=1.25T_{c0}$): (a) $\tau_T\ll\tau_0=10^2\tau_h$, (b) $\tau_T\ll\tau_0=\tau_h$, and (c) $\tau_T\ll\tau_h=10^2\tau_0$.

3.3. The case $\tau_T\ll\tau_0,\tau_h$

Setting $\dot{T}=0$ in (3), we arrive at the relationship (32) in dimensionless form:

$$T=\theta-\eta h.$$

Substituting this in Eq. (2) yields Eq. (34), and Eq. (1) assumes the form (cf. Eq. (33))

$$\dot{\eta}=-\eta\left[1+\frac{\kappa}{1+\eta^2/\alpha^2}\right]+h. \tag{58}$$

As with second-order phase transitions, the system of equations (34) and (58) has a singular point $D(0,0)$ for which the Lyapunov exponent is defined by Eq. (36) where $\theta_c+\tau^{-1}$ and $\theta-\theta_c$, with $\theta_c\equiv 1+\kappa$, must be substituted for $1+\tau^{-1}$ and $\theta-1$, respectively. For $\theta<\theta_c$ this point is a stable node and for $\theta>\theta_c$ it is a saddle point.

Numerical treatment of the phase portrait leads to the situation depicted in Fig. 9. Comparison with the corresponding portrait for a second-order phase transition (see Fig. 5) shows that, as before, the only complication lies in

the appearance of an additional separatrix in the region of small values of h and of η.

In studying a second-order phase transition in Sec. 2.3 we noted that a characteristic feature of the given case is the universality of the system's kinetic behavior manifesting itself not only in the $\tau_h \ll \tau_0$ limit (Fig. 9a) but also in the opposite case $\tau_h \gg \tau_0$ (Fig. 9c), where, it would seem, oscillations should appear. The point is that the curvatures of the parabolas along the h and η axes are determined by the values of the respective reciprocal susceptibilities $\chi_h^{-1} \propto \tau_h^{-1}|\theta - \theta_c|$ and $\chi_\eta^{-1} \propto \tau_0^{-1}|\theta - \theta_c|$, which vary with temperature in a similar manner. Hence, notwithstanding the temperature dependence of the susceptibilities χ_h and χ_η for $\tau_h \gg \tau_0$, the inequality $\chi_h^{-1} \ll \chi_\eta^{-1}$ which implies that the curvature of $V(\eta,h)$ along the h axis is much smaller than along the η axis, still holds. For this reason the trajectories in Fig. 9c along which image points slide down into the "mainstream" are directed practically along the η axis.

4. CONCLUSION

The above investigation shows that the system of Lorentz equations (1)–(3) makes it possible to represent the main features of a phase transition. A thermodynamic description is achieved by using the dependence of the synergetic potential on the order parameter $V(\eta)$. In the case of a second-order phase transition, this dependence has the form (8) and its nature is determined by the control parameter $\theta \equiv T_0/T$: for $\theta < 1$ we have a monotonically increasing V vs η dependence with the minimum at point $\eta_0 = 0$, while for $\theta > 1$ the minimum corresponds to the ordered phase characterized by an order parameter (10). The transition to the case of a first-order phase transition occurs if we assume that the relaxation time of the order parameter acquires a dependence on η according to (41). Then the function $V(\eta)$ is of the form (42), where in comparison to (8) we have introduced two new parameters, κ and η_τ. According to (44), κ determines the renormalization of the critical value of the control parameter, and η_τ specifies the ratio $\alpha \equiv \eta_\tau/\eta_m$. The V vs η dependence has an energy barrier inherent in a first-order phase transition, a barrier that separates the ordered- and disordered-phase minima, provided that $\alpha < 1$. In this case, in the interval (T_c^0, T_c) defined by (43) and (44) the phase transition is of first order, while for $T_0 > T_c$ it is of second. The equilibrium value of the order parameter is determined by Eqs. (45) and (46).

As noted in the introduction, the significant difference between a synergetic phase transition and a thermodynamic phase transition is that the steady-state value of the control parameter corresponding to the medium's temperature T^0 does not coincide with the value of T_0 fixed by the thermostat. For a second-order phase transition this value is the critical temperature T_c specified by (9). The same situation arises in a first-order phase transition for $T_0 \geqslant T_c$, while in the interval $T_c^0 < T_0 < T_c$ the temperature T_+ (see Eq. (48)) corresponding to the maximum in the V vs η dependence is found. Since T_c and T_+ are the minimum values of the control parameter at which ordering begins, the above means that the negative feedback between the order parameter and the conjugate field, reflected by the last term on the right-hand side of Eq. (3), reduces the control parameter so much that only in the limit does it ensure ordering in the medium. What is interesting here is that while in the region $T_0 \geqslant T_c$ the temperature $T^0 = T_c$ of the medium is independent on the thermostat temperature T_0, for a first-order phase transition an increase in T_0 from T_c^0 to T_c leads to a smooth increase in T^0 from the minimum value

$$T^0_{\min} = T_{c0}\left[1 + \alpha\sqrt{\frac{\kappa}{1-\alpha^2}}\right]$$

to the maximum value

$$T^0_{\max} = T_c .$$

Since in the important range of values of the parameters α and κ limited by $k_{\min} = \alpha^2/(1-\alpha^2)$ the minimum temperature $T^0_{\min}$ of the medium is lower than the minimum thermostat temperature T_c^0 in the (T_c^0, T_c) interval the temperature T^0 of the medium is always lower than its value for the thermostat, T_0. At $T_0 = T_c$ the temperatures are equal, and for $T_0 > T_c$ we again have $T_0 > T^0 \equiv T_c$.

The kinetic pattern of the phase transition is represented by the phase portraits shown in Figs. 1, 2, and 4–9 and the time dependence of the path traveled by the image point along a trajectory (Fig. 3). In the case of a second-order phase transition (Figs. 1, 2, 4 and 5) the phase portrait for $T_0 < T_c$ has an attractive node D corresponding to the disordered phase; for $T_0 > T_c$ the node becomes a saddle point and an additional node/focus O corresponding to the ordered phase appears. In contrast, in the phase portrait of a first-order phase transition (Figs. 6–9) a bifurcation appears at $T_0 = T_c^0$ and as result of this a saddle point S, corresponding to the energy barrier in the V vs η dependence, and an attractive node/focus O, corresponding to the ordered phase, appear; the attractive node D of the disordered phase remains unchanged. As the control parameter grows in the (T_c^0, T_c) interval the saddle point S shifts toward the node D and absorbs the node at point T_c, while the node/focus O shifts to higher values of the order parameter and the conjugate field.

The type of singular point O corresponding to the order phase depends on the relationship between τ_η, τ_h, and τ_T.[4)] Obviously, if these relaxation times are incommensurate, the following six characteristic modes can be specified:

$$\begin{aligned}
&\text{(a)}\ \tau_h \ll \tau_T \ll \tau_h, \quad \text{(b)}\ \tau_\eta \ll \tau_T \ll \tau_h,\\
&\text{(c)}\ \tau_T \ll \tau_h \ll \tau_\eta, \quad \text{(d)}\ \tau_T \ll \tau_\eta \ll \tau_h,\\
&\text{(e)}\ \tau_h \ll \tau_\eta \ll \tau_T, \quad \text{(f)}\ \tau_\eta \ll \tau_h \ll \tau_T.
\end{aligned} \tag{59}$$

The above analysis shows that in the cases (a)–(d) the point O is an attractive node, and after a short time interval the trajectory of the system reaches the universal section (the mainstream), whose position is determined by the external conditions (the value of T_0). This represents the universality of the kinetic pattern of a phase transition discovered by Zel'tser *et al.*[6] As the phase portraits show, the mainstream is positioned in the parameter space η, h, T in such a way that when projected on the T, η and T, h planes it has the shape of a monotonically decreasing curve of type MOD in Fig. 2*a* (a

second-order phase transition) or of type MOS in Fig. 7*a* (a first-order phase transition). The projection on the h,η plane is close to the bisectrix (see Figs. 5a and 9a). In addition, for a first-order phase transition a universal section NSP corresponding to the transition of the system appears across the energy barrier (Figs. 6–9). The phase portraits indicate that with the incommensurate nature of the relaxation times in modes (a)–(d) the universal section is reached by traveling along almost straight trajectories that are practically parallel to the axes and correspond to minimum relaxation times. For instance, in mode (a) the image point first moves very rapidly along a straight line parallel to the h axis, then along a section parallel to the T axis with a rate τ_T/τ_h times lower than that along the previous section but τ_η/τ_T times higher than that along the subsequent universal section. As a result it lands in the universal section.

When the relationships between the relaxation times correrspond to modes (e) and (f), the system undergoes damped oscillations in the plane corresponding to the two smallest relaxation times. A characteristic feature of these modes is that in both cases the relaxation time τ_T corresponding to the control parameter is the greatest of the three. As noted in Sec. 3.1, the reason for damped oscillations setting in in the system is the critical increase in the relaxation times τ_η and τ_h according to a law of the form (11). Near the critical point θ_c this increase ensures the commensurability of $\tau_\eta|\theta-\theta_0|^{-1}$ and τ_T in mode (e) and of $\tau_h|\theta-\theta_0|^{-1}$ and τ_T in mode (f), and as a result the relationships between the corresponding parameters η,T and h,T acquire a resonant nature. As for the evolution along the h and η axes, corresponding in modes (e) and (f) to shortest relaxation times, it retains the same nature as when the universal section is reached: the system moves into the corresponding plane along the perpendicular axis with a rate that is τ_T/τ_h (mode (e)) or τ_T/τ_η (mode (f)) times higher than the oscillation frequency.

Just as we did in Sec. 3.1 when analyzing the particular case of $\tau_h \ll \tau_0,\tau_T,$, we can clarify the behavior of the kinetic behavior by analyzing the dependence of the synergetic potential V on the complete set of parameters η, h, and T. Since the main contribution to the universal behavior of the system is provided by the neighborhoods of the extrema in this dependence, characterized by the coordinates η_e, h_e, and T_e, in the quadratic approximation we have the following expression:

$$V \approx V(\eta_e,h_e,T_e)+\frac{\chi_\eta^{-1}}{2}(\eta-\eta_e)^2+\frac{\chi_h^{-1}}{2}(h-h_e)^2 + \frac{\chi_T^{-1}}{2}(T-T_e)^2, \tag{60}$$

where χ_η, χ_h, and χ_T are the susceptibilities determining the curvature of the dependence of V on η, h, and T along the corresponding axes. Since these susceptibilities are proportional to the corresponding effective relaxation times of type (11), we can write

$$\chi_\eta \propto \tau_\eta|\theta-\theta_c|^{-1}, \quad \chi_h \propto \tau_h|\theta-\theta_c|^{-1}, \quad \chi_T \propto \tau_T. \tag{61}$$

Characteristically, the values of the susceptibilities χ_η and χ_h corresponding to the order parameter and the conjugate field increase without limit in the neighborhood of the critical point θ_c, while the value of the susceptibility χ_T corresponding to the control parameter is temperature-independent. Hence for the three-dimensional paraboloid (60) the hierarchy (59) of the relaxation times does not always ensure that the curvatures of the paraboloid (60) along the different axes are incommensurate. In particular, in the critical region the following may be true:

$$\begin{aligned}&\text{(a)}\ \chi_h^{-1} \gg \chi_T^{-1} \gg \chi_\eta^{-1}, \quad \text{(b)}\ \chi_\eta^{-1} \gg \chi_T^{-1} \gg \chi_h^{-1},\\ &\text{(c)}\ \chi_T^{-1} \gg \chi_h^{-1} \gg \chi_\eta^{-1}, \quad \text{(d)}\ \chi_T^{-1} \gg \chi_\eta^{-1} \gg \chi_h^{-1},\\ &\text{(e)}\ \chi_h^{-1} \gg \chi_\eta^{-1} \sim \chi_T^{-1}, \quad \text{(f)}\ \chi_\eta^{-1} \gg \chi_h^{-1} \sim \chi_T^{-1},\end{aligned} \tag{62}$$

and in modes (e) and (f) the curvatures of the paraboloid (60) become pairwise commensurate. This means that near the ordered-phase minimum the $V(\eta,h,T)$ dependence in the T,η and T,h planes becomes a paraboloid of revolution with a curvature much smaller than along the perpendicular axes (h and η, respectively). As a result the image point not only slides down into the minimum of this paraboloid but is also in rotational motion on the paraboloid's surface. The rotation corresponds to the damped oscillations in the T,η plane (mode (e)) and in the T,h plane (mode (f)).

Note that this critical decrease in curvature has an effect only near the ordered-phase minimum and is not present near the energy barrier. Hence the phase portraits in Figs. 7*c* and 8*c* suggest that notwithstanding the fact that the trajectories near the point O are twisted, a change in the relaxation-time ratio has no effect on the separatrix near the saddle point S.

As for the modes (a)–(g), here the critical behavior of the system does not disrupt the hierarchy (62) of the curvatures χ^{-1} caused by the inequalities (59) between the relaxation times τ, and the system behavior rapidly becomes universal. For instance, in mode (a), where the curvature χ_h^{-1} is the greatest and the curvature χ_η^{-1} the smallest, the image point very rapidly slides down the surface specified by the $V(\eta,h,T)$ dependence along the h axis or less rapidly along the T axis, and then moves smoothly along the universal section. In other words, in the (a)–(d) modes the surface $V(\eta,h,T)$ has the shape of a narrow trough whose bottom coincides with the universal trajectory. The fact that the universal trajectory is not parallel to the axis corresponding to the smallest curvature χ^{-1} means that the extremum values along the other axes depend on the respective parameters. For instance, in mode (a) the extremum value of the conjugate field, $h_e(\eta)$, and that of the control parameter, $T_e(\eta)$, acquire in time τ_T a functional dependence of the form (4) and (5) on the order parameter.

As is well known,[12] a remarkable feature of the Lorentz system is that it describes a strange attractor in which the universal trajectory represents a fractal, a set of fractional dimensionality (see Ref. 13). Clearly, the two-dimensional damped oscillations discovered in modes (e) and (f) correspond to the sections of the strange attractor by the T,η and T,h planes (but are not reduced to these sections). To proceed from these oscillations to the strange-attractor mode we

must include the motion along the perpendicular axis (the h axis in mode (e) and the η axis in mode (f)). The appropriate relationships in (59) show that this can be achieved only if the corresponding relaxation times are comparable: $\tau_h \sim \tau_\eta$. Thus, a transition to the strange-attractor mode should be expected if

$$\tau_h \sim \tau_\eta \ll \tau_T, \quad \chi_h \sim \chi_\eta \sim \chi_T. \tag{63}$$

If the ratio $\tau \equiv \tau_h / \tau_\eta$ is varied, in the $\tau \ll 1$ limit the strange attractor degenerates into oscillations in the T, η plane, while in the opposite limit $\tau \gg 1$ these oscillations appear in the T,h plane. But if the ratio $\tau_T / \tau_{\eta,h}$ decreases, the frequency of oscillations in the corresponding plane decreases, too.

In conclusion we discuss the nature of these approximations. First, we must bear in mind that the Lorentz system we employed describes phase transitions induced by noise, and ordering in such transitions emerges when the intensity of the noise caused by the stochastic action of an external medium (the thermostat) increases.[14] An example of this type of transformation is the phase transition induced by a growth in pressure, which in this case acts as the control parameter (see Ref. 15). In equilibrium thermodynamic systems the temperature acts as the noise intensity (see Ref. 2), in view of which everywhere above we adopted the value of T as the magnitude of the control parameter. One must bear in mind, however, that ordering in thermodynamic systems occurs at small values of the control parameter rather than at large.[11] Hence, as applied to such systems the control parameter corresponds not to the temperature but to its reciprocal value. We note in this connection that a derivation of thermodynamic relationships based on the Gibbs distribution presupposes the use of the reciprocal temperature (see Ref. 11).

Another essential limitation of our approach is the fact that the systems we studied were spatially homogeneous, although in the case of a conserved order parameter an inhomogeneous structure is always formed in the process of transition.[1,2] Two markedly different behavior patterns should be distinguished here: the binodal and the spinodal. In thermodynamic systems the first corresponds to the supercritical region and the second to the subcritical. The transition between the two represents a loss of ergodicity of the stochastic system in the binodal region, the loss being related to the emergence of sharp interphase (antiphase) boundaries.[16]

One can easily see that in the spinodal region, where the coordinate dependence of the system parameters is smooth, allowing for this dependence presents no difficulties. Indeed, if we go from the coordinate representation to the wave representation, we only need to introduce into the initial relaxation times the factors $(1+\xi^2\mathbf{k}^2)^{-1}$ dependent on the wave vector $\mathbf{k}$, where ξ is the correlation length corresponding to the given parameter. In the binodal region, besides ξ there appear additional scales L characterizing the macrostructure (see the Introduction), and the situation becomes much more complicated.[1,2] Its study constitutes a separate problem.

The authors would like to express their gratitude to the Ukrainian State Committee for Science and Technology for supporting their work (Grants Nos. 2.2/205 and 2.3/82). They are also grateful to the participants of the Synergetics Seminars held at the Moscow State University and the Institute of Physics of the National Academy of Sciences of the Ukraine for discussing the results of the present work

[1)] If the order parameter corresponds to spontaneous magnetization, the conjugate field is reduced to magnetic induction. For ordered solid solutions, where the order parameter determines the long-range order in the alteration of atoms of different species, the conjugate field is the difference of the chemical potentials of the components.

[2)] Since the value of η_0 is restricted by the condition $\eta_0 \leqslant \eta_m$, the excitation parameter θ is bounded from above by the value $\theta_m = 2$

[3)] This follows from the fact that the curvature is inversely proportional to the corresponding susceptibility, which in turn is proportional to the corresponding relaxation time.[10]

[4)] For a first-order phase transition, τ_η must be interpreted as the relaxation time τ_0 in Eq. (41).

[1] A. J. Bray, Adv. Phys. **43**, 357 (1994).
[2] A. I. Olemskoĭ and I. V. Koplyk, Usp. Phys. Nauk **165**, 1105 (1995).
[3] A. Z. Patashinskiĭ and V. L. Pokrovskiĭ, *Fluctuation Theory of Phase Transitions*, Pergamon Press, Oxford (1979).
[4] I. M. Lifshits, Zh. Éksp. Teor. Fiz. **42**, 1354 (1962) [Sov. Phys. JETP **15**, 939 (1962)].
[5] I. M. Lifshits and V. V. Slezov, Zh. Éksp. Teor. Fiz. **35**, 479 (1958) [Sov. Phys. JETP **8**, 331 (1959)].
[6] A. S. Zel'tser, T. K. Soboleva, and A. É. Filippov, Zh. Éksp. Teor. Fiz. **108**, 356 (1995) [JETP **81**, 193 (1995)].
[7] H. Haken, *Synergetics. An Introduction. Nonequilibrium Phase Transitions and Self-Organization in Physics, Chemistry, and Biology*, 3 rd ed., Springer, Berlin (1983).
[8] A. I. Olemskoĭ and V. A. Petrunin, Izv. Vyssh. Uchebn. Zaved. Fiz. No. 1, 82, (1987) [in Russian].
[9] A. A. Andronov, A. A. Vitt, and S. É. Khaĭkin, *Theory of Oscillations* [in Russian], Nauka, Moscow (1981); an earlier edition of this book was translated at Pergamon Press, Oxford (1966).
[10] A. A. Katsnel'son and A. I. Olemskoĭ, *Microscopic Theory of Inhomogeneous Media* [in Russia], Moscow Univ. Press, Moscow (1987).
[11] L. D. Landau and E. M. Lifshitz, *Statistical Physics*, Part 1, 3 rd ed., Pergamon Press, Oxford (1980).
[12] H. Haken, *Advanced Synergetics. Instability Hierarchies of Self-Organizing Systems and Devices*, Springer, Berlin (1987).
[13] A. I. Olemskoĭ, in *Physics Reviews*, edited by I. M. Khalatnikov, Vol. 18, Part 1, Gordon and Breach, London (1996), p. 1; A. I. Olemskoĭ and A. Ya. Flat, Usp. Fiz. Nauk **163**, No. 12, 1 (1993) [Phys. Usp. **36**, 1087 (1993)].
[14] W. Horsthemke and R. Lefever, *Noise-Induced Transitions. Theory and Applications in Physics, Chemistry, and Biology*, Springer, Berlin (1984).
[15] A. I. Olemskoĭ and I. A. Sklyar, Usp. Fiz. Nauk **162**, No. 6, 29 (1992) [Phys. Usp. **35**, 455 (1992)].
[16] A. I. Olemskoĭ, E. A. Toropov, and I. A. Sklyar, Filippov, Zh. Éksp. Teor. Fiz. **100**, 987 (1991) [Sov. Phys. JETP **73**, 545 (1991)].

Translated by Eugene Yankovsky